Supplementary Information for:

Functionalization of Maleimide-Coated Silver Nanoparticles through Diels-Alder Cycloaddition

Cheng Chen and Ljiljana Fruk*

Karlsruhe Institute of Technology, Centre for Functional Nanostructures, 76131 Karlsruhe, Germany. Fax: +49 (0) 721 608 48496; Tel: +49 (0) 721 608 45800; E-mail: ljiljana.fruk@kit.edu

1. Chemicals and Instruments

All chemicals and DNA oligonucleotides were purchased from Sigma Aldrich, except for 5-aminobenzotriazole (Alfa Aesar), and used without further purification. Milli-Q water was used throughout the experiments. The TEM images were taken by using a Philips CM200 FEG/ST electron microscope. The fluorescence spectra were recorded on a CARY Eclipse fluorescence spectrophotometer (Varian) and UV-Vis absorption spectra on a CARY50 UV-Vis spectrophotometer (Varian). High-performance liquid chromatography (HPLC) purification was performed on an Agilent 1200 series HPLC system. The fast protein liquid chromatography (FPLC) was performed on a GE ÄKTA^{TM} Explorer 900 FPLC system. The image of gel electrophoresis was taken by a Bio-RAD Gel Doc^{TM} XR imaging system.

2. Synthesis of Benzotriazole-Maleimide (BTM)

3-(1H-Benzotriazol-5-ylcarbamoyl)acrylic acid (**1**)

10 mmol 5-amino-benzotriazole (amino-BT) was partially dissolved in 50 mL dichloromethane (DCM). 20 mmol maleic acid anhydride was dissolved in 10 mL DCM and added to the above solution portionwise over half an hour. The reaction mixture was stirred at room temperature (RT) overnight. The grey precipitate was collected by filtration, washed with DCM and dried to give the title compound **1** in 88% yields. R_f (DCM-MeOH 9:1) 0.0; ^{1}H NMR (250 MHz) δ_H(DMSO-d_6): 6.34 (1H, d, *J* 12.5, C*H*CHCO$_2$H), 6.53 (1H, d, *J* 12.5, CHC*H*CO$_2$H), 7.41 (1H, br s, H-7), 7.92 (1H, br s, H-4), 8.36 (1H, br s, H-6), 10.6 (1H, s, CO$_2$*H*); m/z (FAB) for $C_{10}H_8N_4O_3$ $[M+H]^+$: 233.2.

1-(1H-Benzotriazol-5-yl)pyrrole-2,5-dione (BTM) (**3**)

7.5 mmol anhydrous sodium acetate was dissolved in 125 mL acetic anhydride and 6.3 mmol compound **1** was added. The mixture was refluxed and stirred at 90 ℃ for 4 h. After removing the acetic anhydride by rotary evaporator, the residue (compound **2**) was dissolved in 10 mL trifluoroacetic acid (TFA) and the mixture was stirred at RT overnight. After the removal of TFA in vacuo, cold H_2O was added and the precipitate was collected by filtration, washed with ethanol and dried. The product was purified by column chromatography eluting with EtOAc in hexane (10–70%) to give the title compound **3** as a yellow powder in 50.7% yield. R_f (DCM-MeOH 9:1) 0.18; ^{1}H NMR (250 MHz) δ_H(DMSO-d_6): 7.23 (2H, s, C*H*=C*H*), 7.40 (1H, d, *J* 7.5, H-7), 7.89 (1H, s, H-4), 8.01 (1H, d, *J* 7.5, H-6); m/z (FAB) for $C_{10}H_6N_4O_2$ $[M+H]^+$: 215.1.

3. Synthesis of BTM-Coated Ag NPs

Certain amount of BTM and 0.002 mmol $AgNO_3$ were dissolved in the mixure of MeCN and H_2O (v: v = 2: 3). Different ratios between BTM and $AgNO_3$ (10:1, 30:1, 50:1, 80:1 and 100:1) were tried. The mixture was stirred in ice-bath for 1 h to achieve a chelating balance, after which 2 mL freshly prepared $NaBH_4$ solution (5 mM) was added dropwise. The reaction was stirred in ice-bath for 1 h. The NPs were characterized by TEM. As indicated by Fig. S1, bigger nanoparticles or nanoflowers formed when the amount of BTM was low. With the increase of the amount of BTM, the BTM molecules would prevent the aggregation of the small NPs and thus afford relatively monodispersed Ag NPs. The BTM-coated Ag NPs, which

were obtained when 100 equivalents BTM were used, were measured by UV-Vis and fluorescence spectrometer (Fig. S2) and used for the further functionalization.

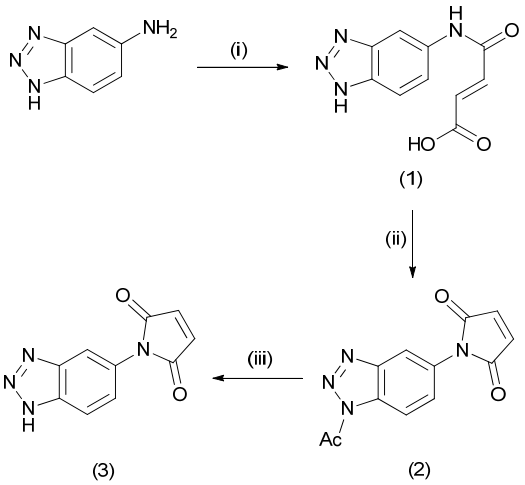

Scheme S1 Synthetic procedures of BTM. Reagents and conditions: (i) maleimide anhydride, CH_2Cl_2, RT, overnight; (ii) acetic anhydride, 90 ºC; (iii) TFA, RT, overnight.

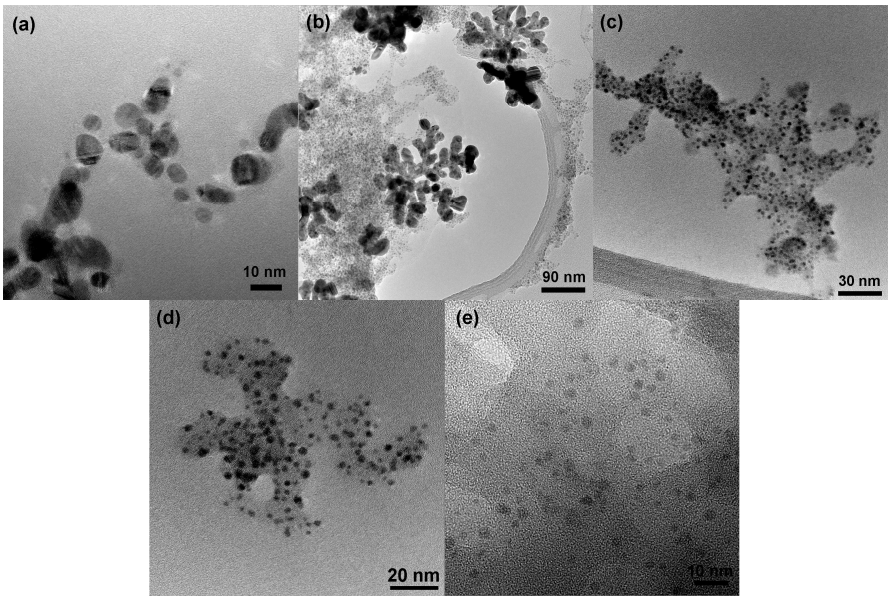

Fig. S1 TEM images of BTM-Ag NPs obtained at different ratios between BTM and $AgNO_3$. (a) 10:1, (b) 30:1, (c) 50:1, (d) 80:1 and (e) 100:1

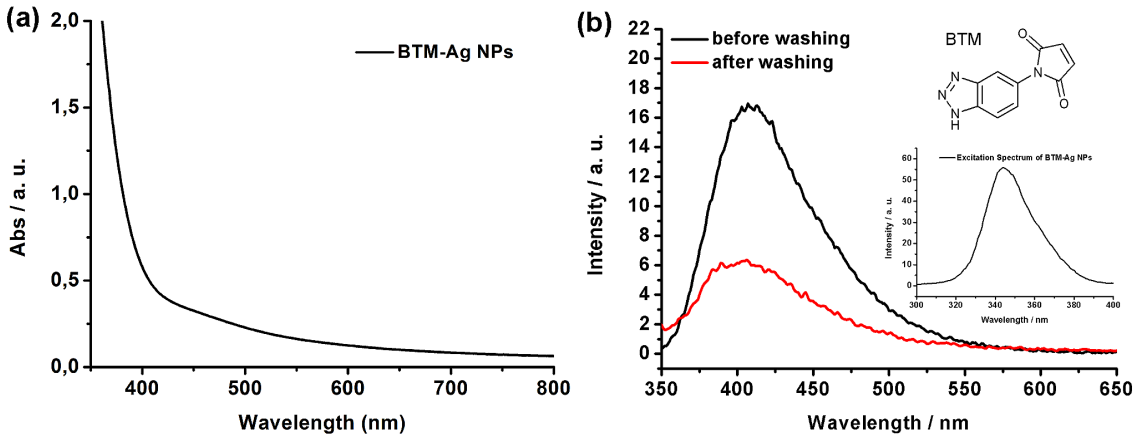

Fig. S2 (a) UV-Vis and (b) fluorescence spectra of BTM-Ag NPs (inset of b: excitation spectrum of BTM-Ag NPs)

4. Franck-Condon Principle in Solvation

According to the Franck-Condon principle in solvation (Fig. S3b)[24], the dipole moments of the polar solvent molecules could interact with the dipole moment of the fluorophore. In the ground state, the solvent molecules are oriented in such a way that their dipole moments compensate for the dipole moment of the fluorophore in order to minimize the total energy of the whole system. After excitation, electronic transition to higher energy level leads to the change in the dipole moment of fluorophore, which ultimately induces the reorientation of the solvent molecules. The solvent relaxation around the excited fluorophore cause the decrease of the energy separation between the ground and excited states, which results in the increase of electronic transition probability and finally lead to the enhancement of the fluorescence intensity. Therefore, increasing the solvent polarity will correspondingly cause a larger decrease in the energy gap between the ground and excited states. Since the polarity of H_2O is higher than that of MeCN (polarity parameter: H_2O 10.2 and MeCN 5.8), so that the fluorescence intensity of BTM could be enhanced when H_2O appeared in the solvent system.

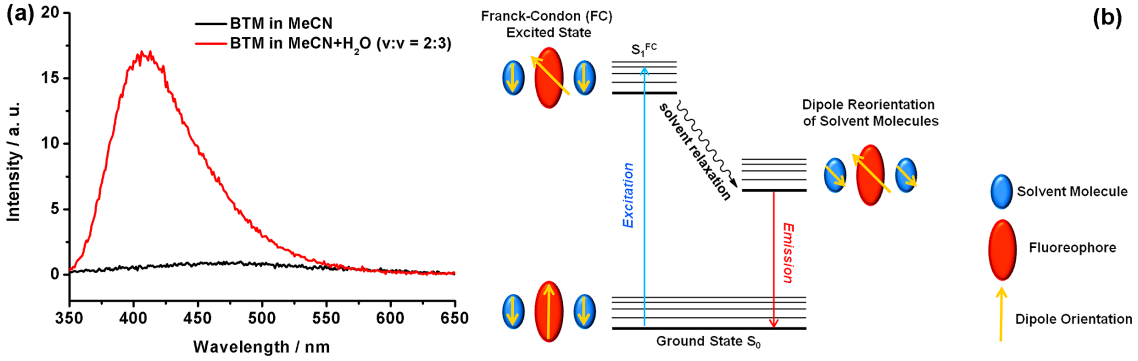

Fig. S3 (a) Fluorescence spectra of BTM in different solvents and (b) Illustration of Franck-Condon principle in solvation

5. Analyses of BTM after Being Heated at 60 °C

BTM was first analyzed by ^{1}H NMR and MS after being heated at 60°C overnight. ^{1}H NMR (250 MHz) δ_H(DMSO-d_6): 6.34 (0.14 H d, *J* 12.5, C*H*CHCO$_2$H), 6.52 (0.07 H d, *J* 12.5, CHC*H*CO$_2$H), 7.21 (2H, s, C*H*=C*H*), 7.41 (1H, d, *J* 10.0, H-7), 7.89 (1H, s, H-4), 8.01 (1H, d, *J* 5.0, H-6), 8.34 (0.07 H, br s, H-6), 10.6 (0.07 H, s, CO$_2$*H*); m/z (ESI) for $C_{10}H_6N_4O_2$ $[M+H]^+$ 215.25 and $C_{10}H_8N_4O_3$ $[M+H]^+$ 233.17. The results show that traces of compound **1** formed, which indicate that maleimide could undergo ring opening hydrolysis when BTM is heated to 60°C in aqueous solution. By comparing the fluorescence spectra of BTM and compound **1** (Fig. S5), we could know that the fluorescence of compound **1** is not higher than that of BTM, so that it was not responsible for the increase of fluorescence.

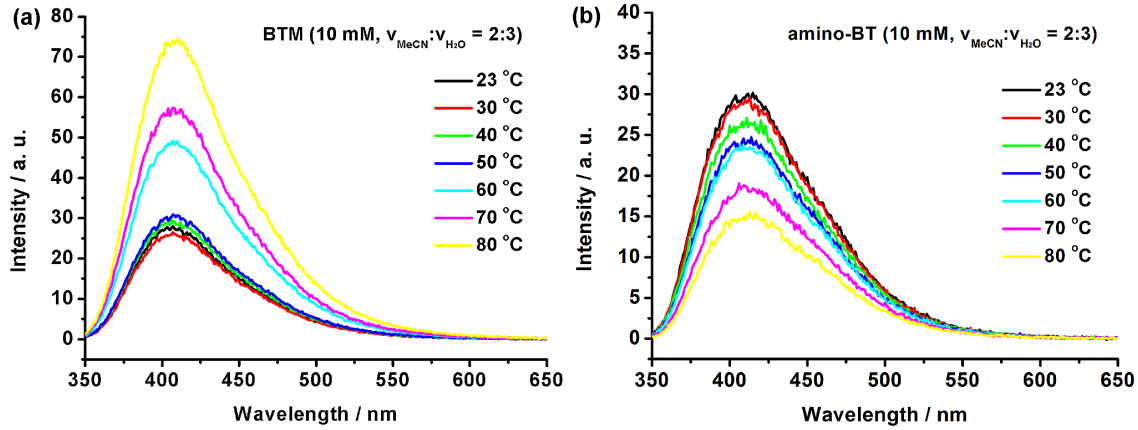

Fig. S4 Fluorescence spectra of (a) BTM and (b) amino-BT in the mixture of MeCN and H_2O at different temperatures

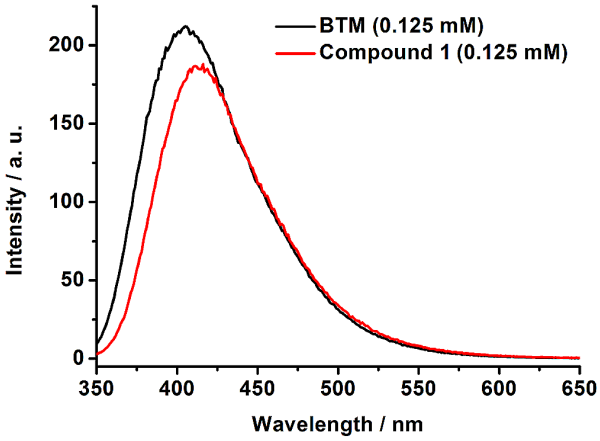

Fig. S5 Fluorescence spectra of BTM and Compound **1**

In order to investigate further into the reasons for the significant fluorescence enhancement of BTM after being heated at 60 °C, UV-Vis spectra of BTM and amino-BT were measured at 23 and 60 °C (Fig. S6). The absorption peak of BTM (23 °C) at 300 nm could be attributed to the 2-*H* tautomer of BTM, while the other peak around 260 nm belongs to the 1-*H* tautomer of BTM (Scheme S2).[1] After being heated at 60 °C, the peak at 300 nm decreased and the peak at 260 nm increased, which indicate that part of 2-*H* BTM transformed to 1-*H* BTM. On the contrary, the ratio between the two absorption peaks of amino-BT didn't change obviously, which might because there was no big change in the ratio between 1-*H* tautomer and 2-*H* tautomer of amino-BT. To further prove this, Fourier transform infrared spectroscopy (FTIR) was used to analyze the structures of BTM and amino-BT before and after being heated at 60 °C. Compared with the FTIR spectrum of BTM (23 °C) (Fig. S7a), a new band appeared at 3507 cm^{-1} in the spectrum of BTM (60 °C) (Fig. S7b), which could be assigned to the N-H stretching vibration of the 1-*H* BTM.[2] There is no obvious change in the FTIR spectra of amino-BT (23 and 60 °C) (Fig. S7c and d). The structural information given by FTIR is in coordination with the UV-Vis analyses. According to the above results, we deduce that the fluorescence enhancement of BTM upon heating might be caused by the tautomerization of BTM.

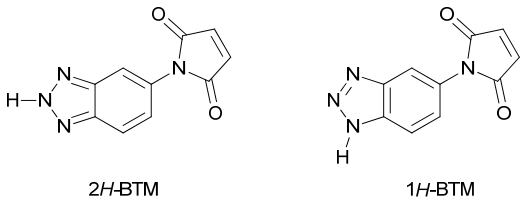

Scheme S2 The 2-*H* and 1-*H* tautomers of BTM

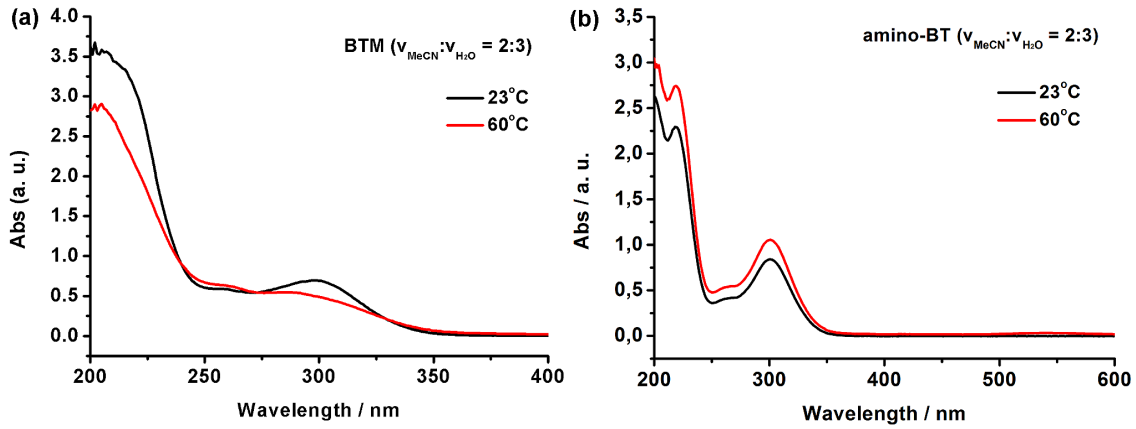

Fig. S6 UV-Vis spectra of BTM and amino-BT at 23°C and 60°C

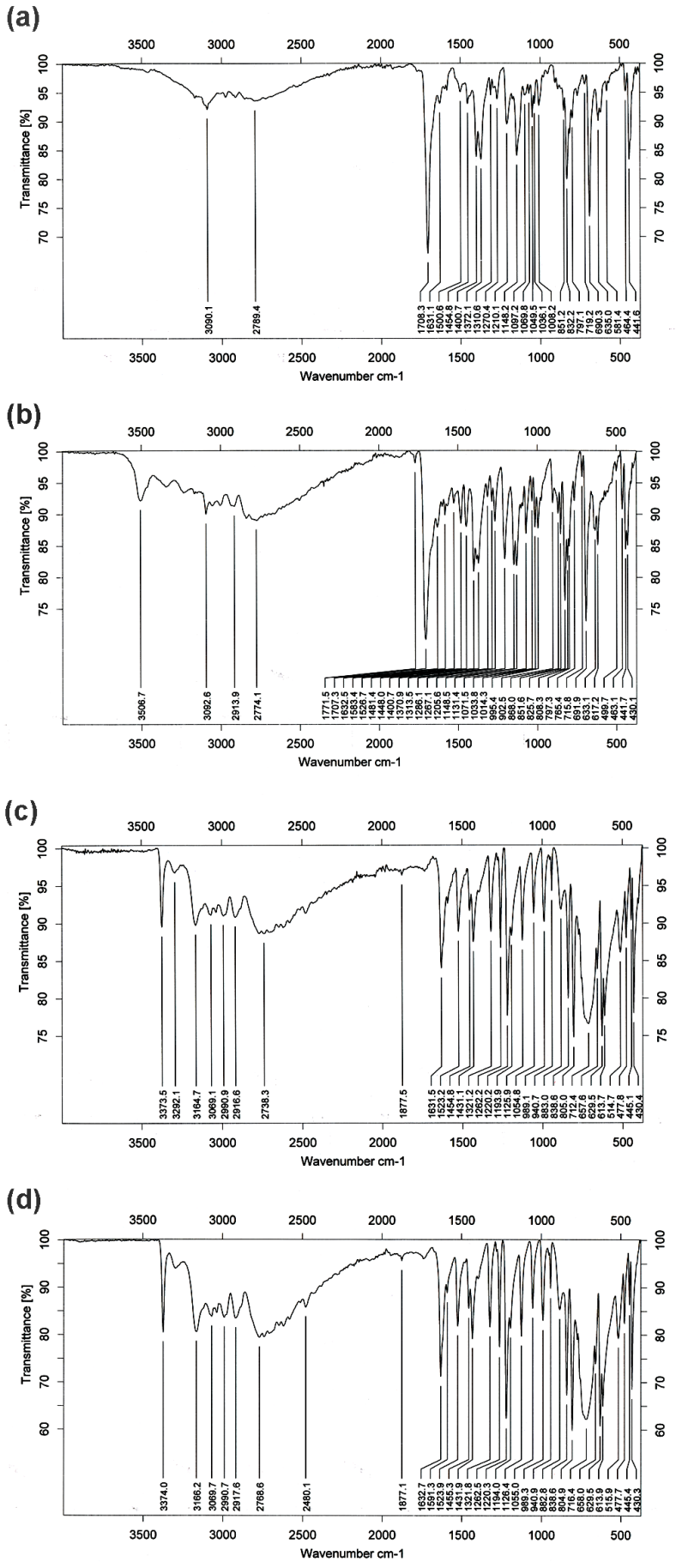

Fig. S7 FTIR spectra of (a) BTM 23ºC, (b) BTM 60ºC, (c) amino-BT 23ºC and (d) amino-BT 60ºC

6. Preparation of Furan-Modified *ss*DNA

(1) Synthesis of *N-Furan-2-ylmethyl succinamic acid* (**4**)

Succinic anhydride (17 mmol) was dissolved in DCM (10 mL) and added to furfurylamine (1.0 mL, 10 mmol) dropwise and the reaction mixture stirred for 3 h at RT. The title compound **4** was collected by filtration, washed with DCM and dried. R_f (DCM-MeOH 9:1) 0.12; ^{1}H NMR (250 MHz) δ_H(DMSO-d_6) 2.34 (2H, t, *J* 5.0, COCH_2), 2.43 (2H, t, *J* 5.0, CH_2CO_2H), 4.22 (2H, d, *J* 5.0, CH_2NH), 6.21 (1H, s, Fur-*H*), 6.36 (1H, s, Fur-*H*), 7.55 (1H, s, Fur-*H*), 8.29 (1H, s, CO_2*H*), 12.07 (1H, br s, N*H*CO); m/z (FAB) for $C_9NO_4H_{11}$ $[M+H]^+$: 198.1.

(2) Preparation of Furan-Modified *ss*DNA

0.03 mmol compound **4** was activated with 0.06 mmol 1,1'-carbonyl diimidazole (CDI) in anhydrous DMF (0.25 mL) at 45 ^{o}C for 5 min. Then 10 nmol amino-modified 12-base *ss*DNA oligonucleotide (5'-GGC GTA TAA CAA) was added. The solution was incubated at 37 ^{o}C overnight and the product was purified by HPLC using linear gradient of buffer B over 45 min (buffer A: ammonium acetate, buffer B: acetonitrile) (Fig. S8a). The formation of furan-modified *ss*DNA was confirmed by matrix-assisted laser desorption/ionization (MALDI) (Fig. S8b).

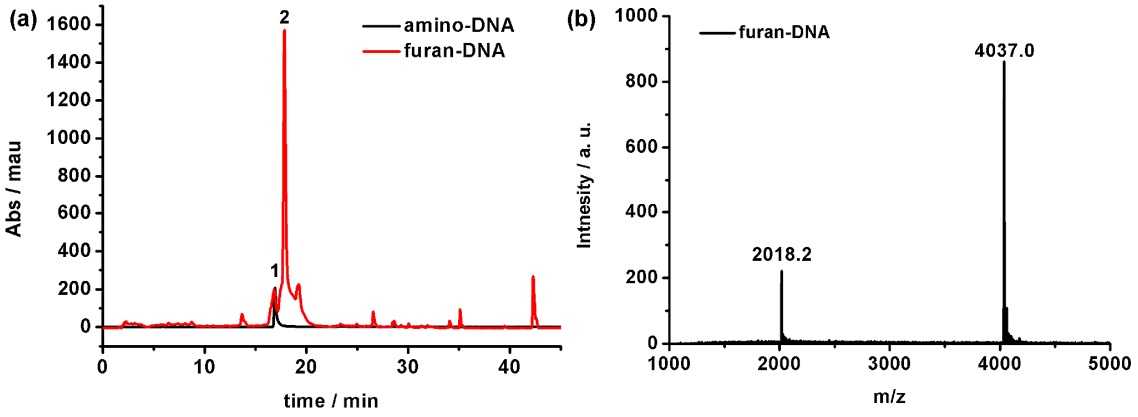

Fig. S8 (a) HPLC chromatogram of furan-modified *ss*DNA: peak 1 is pure amino-modified *ss*DNA and peak 2 is furan-modified *ss*DNA; (b) MALDI spectrum of peak 2

7. Preparation of Mb-*c*DNA Conjugates

100 µL thiol-modified *c*DNA (100 µM) was first reduced with DTT (1 M) at 37 ^{o}C for 2 h. 200 µL nMb solution (200 µM) was incubated with Sulfo-SMCC crosslinker at 23 ^{o}C for 2 h in the dark. The two solutions were desalted by NAP-5 and 10 columns, mixed together directly and incubated at 23 ^{o}C for 3 h. The Mb-*c*DNA conjugates were purified by FPLC with buffer A (20 mM Tris) and gradient of buffer B (20 mM Tris + 1 M NaCl) over 40 min (Fig. S9a). After purification, the fractions were analyzed by UV-Vis spectroscopy (Fig. S9b) and native polyacrylamide gel electrophoresis (Fig. S10). Two different Mb-*c*DNA conjugates (**1** and **2**) were obtained and identified according to their UV-Vis spectra as conjugates containing one and two DNA strands, respectively.

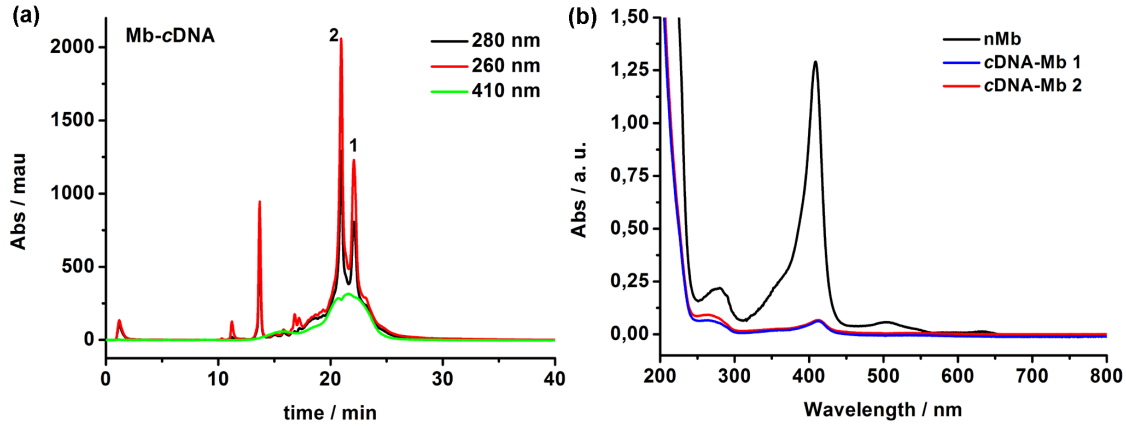

Fig. S9 (a) FPLC chromatogram and (b) UV-Vis spectra of Mb-*c*DNA conjugates

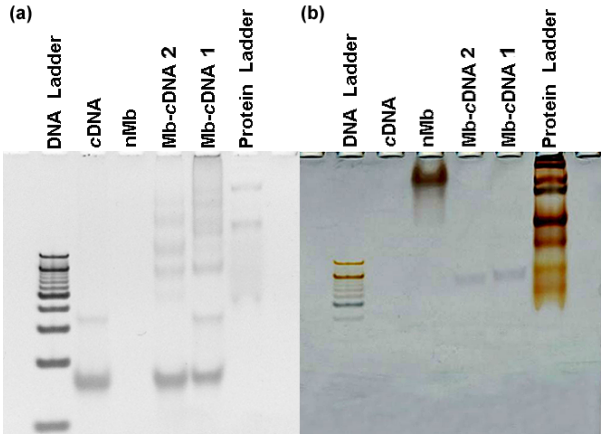

Fig. S10 Gel electrophoresis of Mb-*c*DNA conjugates: (a) SYBR gold stain and (b) silver stain

8. Preparation and Fluorescence of PEG-modified Ag NPs

200 μL BTM-Ag NPs were mixed with 200 μL PEG-CP (200 μM) in the mixture of MeCN and H_2O (v: v = 1: 1). After the addition of 0.3 M LiCl, the solution was incubated at 23°C for 2 h. The formation of PEG-modified Ag NPs was proved by gel electrophoresis. The fluorescence study of PEG-coated Ag NPs before and after heating (Fig. S11) again proved that the intrinsic property of BTM would not be affected by the conjugation upon the maleimide ring.

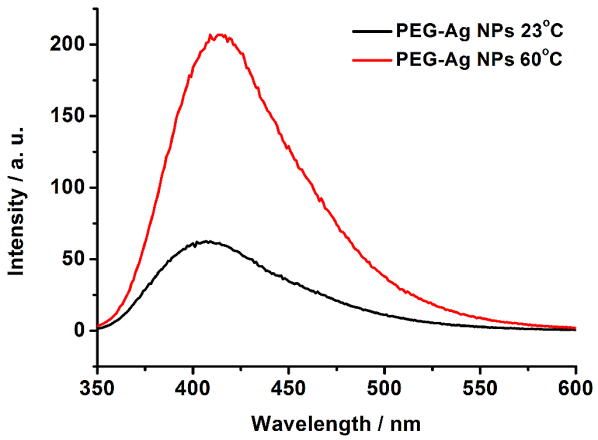

Fig. S11 Fluorescence spectra of PEG-modified Ag NPs at 23 and 60 °C

References

1. A. C. Borin, L. Serrano-Andres, V. Ludwig and S. Canuto, *Phys. Chem. Chem. Phys.*, 2003, **5**, 5001-5009.
2. W. Roth, D. Spangenberg, C. Janzen, A. Westphal and M. Schmitt, *Chem. Phys.*, 1999, **248**, 17-25.